

Article

Assessment of Soil Capability and Crop Suitability Using Integrated Multivariate and GIS Approaches toward Agricultural Sustainability

Radwa A. El Behairy ¹, Ahmed A. El Baroudy ¹, Mahmoud M. Ibrahim ¹, Elsayed Said Mohamed ^{2,3}, Dmitry E. Kucher ³ and Mohamed S. Shokr ^{1,*}

¹ Soil and Water Department, Faculty of Agriculture, Tanta University, Tanta 31527, Egypt; radwa126710stud_pg@agr.tanta.edu.eg (R.A.E.B.); drbaroudy@agr.tanta.edu.eg (A.A.E.B.); mahmoud.abouzaid@agr.tanta.edu.eg (M.M.I.)

² National Authority for Remote Sensing and Space Sciences, Cairo 11843, Egypt; elsayed.salama55@mail.ru

³ Department of Environmental Management, Institute of Environmental Engineering, People's Friendship University of Russia (RUDN University), 6 Miklukho-Maklaya Street, 117198 Moscow, Russia; kucher-de@rudn.ru

* Correspondence: mohamed_shokr@agr.tanta.edu.eg

Abstract: Land evaluation has an important role in agriculture. Developing countries such as Egypt face many challenges as far as food security is concerned due to the increasing rates of population growth and the limited agriculture resources. The present study used multivariate analysis (PCA and cluster analysis) to assess soil capability in drylands, Meanwhile the Almagra model of Micro LEIS was used to evaluate land suitability for cultivated crops in the investigated area under the current (CS) and optimal scenario (OS) of soil management with the aim of determining the most appropriate land use based on physiographic units. A total of 15 soil profiles were selected to characterize the physiographic units of the investigated area. The results reveal that the high capability cluster (C1) occupied 31.83% of the total study area, while the moderately high capability (C2), moderate capability (C3), and low capability (C4) clusters accounted for 37.88%, 28.27%, and 2.02%, respectively. The limitation factors in the studied area were the high contents of CaCO₃, the shallow soil depth, and the high salinity and high percentage of exchangeable sodium (% ESP) in certain areas. The application of OS enhanced the moderate suitability (S3) and unsuitable clusters (S5) to the suitable (S2) and marginally suitable (S4) categories, respectively, while the high suitability cluster (S1) had increased land area, which significantly affected the suitability of maize crop. The use of multivariate analysis for mapping and modeling soil suitability and capability can potentially help decision-makers to improve agricultural management practices and demonstrates the importance of appropriate management to achieving agricultural sustainability under intensive land use in drylands.

Keywords: soil capability index; PCA; GIS; land capability and suitability; cluster analysis; sustainable agriculture



Citation: El Behairy, R.A.; El Baroudy, A.A.; Ibrahim, M.M.; Mohamed, E.S.; Kucher, D.E.; Shokr, M.S. Assessment of Soil Capability and Crop Suitability Using Integrated Multivariate and GIS Approaches toward Agricultural Sustainability. *Land* **2022**, *11*, 1027. <https://doi.org/10.3390/land11071027>

Academic Editors: Chiara Piccini and Rosa Francaviglia

Received: 2 June 2022

Accepted: 4 July 2022

Published: 6 July 2022

Publisher's Note: MDPI stays neutral with regard to jurisdictional claims in published maps and institutional affiliations.



Copyright: © 2022 by the authors. Licensee MDPI, Basel, Switzerland. This article is an open access article distributed under the terms and conditions of the Creative Commons Attribution (CC BY) license (<https://creativecommons.org/licenses/by/4.0/>).

1. Introduction

Worldwide food insecurity is currently one of the most significant challenges facing humanity. Demand for food is expected to rise by 70.00% by 2050, and agricultural productivity is a crucial component of global food security [1]. Rapid population growth has exacerbated global human food insecurity, thus necessitating long-term evaluation of natural resources. It is thought that the world population will be more than nine billion by 2050 [2,3]. As such, it is anticipated that there might be shortages in both agricultural resources and land [4,5]. One possible solution to compensate for this shortage is to encourage increasing crop yields. However, this entails using pesticides and fertilizers that may affect the environment negatively. Another possible solution is to import more crops to fill

the food gap [4,6]. If properly managed, soil is one of the most significant natural resources that can abet in bridging the food demand gap to achieve food security [7]. Agricultural fields in the Nile Valley and Delta, Egypt, account for about 4.00% of the country's total land area [8]. The growth of the agricultural sector in Egypt is considered an important long-term development backbone. The agricultural sector contributes about 14.50% of the gross national product in Egypt and 30.00% of foreign revenue from the export of agricultural products, and has led to a 41.00% decrease in unemployment [9]. Agricultural growth on arable land strives to accomplish long-term agricultural development by the integration of soil, water, and environmental factors [10,11]. The term "land evaluation" refers to the performance rate of the land and its ability for crop production, with the capacity varying according to climate, geographical location, and physiochemical characteristics [12]. Land evaluation can enable decision-makers to select the best-performing crops based on soil properties [11,13]. The soil limiting factors for crop suitability vary in different areas in Egypt, with soil salinity, poor drainage, and compaction as the most common factors in the northern Nile Delta [14–17]. Agriculture is the greatest user of water in Egypt, especially in the northwestern Nile Delta; thus, determining and controlling surface water quality in such areas is vital for protecting water resources and ensuring long-term sustainable agriculture [18]. Soil property characterization, modeling, and mapping at various spatial and temporal scales are required for the study of diverse environments [19]. The Geographic Information System (GIS) technique has accelerated spatial variability studies of different environmental phenomena [20]. Thus, integrating GIS and geostatistical analysis to map and detect the spatial variation of soil parameters in previously unstudied areas might be beneficial. For instance, inverse distance weighted is an interpolation procedure that uses known values with corresponding weighted values to estimate unknown values in a study location [21]. Land capability assessment has a vital role in adequate planning, particularly in arid climate zones [22]. Combining the properties of soil in order to evaluate its capability is limited by the intricate nature of the soil system. Consequently, multivariate analysis has been identified as an appropriate tool for soil capability zone evaluation owing to its ability to perform systematic modeling in unclear and indistinct scenarios [23–25]. PCA and cluster analysis are multivariate procedures that are widely used for soil data recognition, classification, and modeling [26]. Models of soil evaluation, theoretical agricultural management scenarios, and spatial analyses are valuable tools used by land managers and decision-makers to achieve sustainability of land use and management for different studied areas [27,28]. The Micro Land Evaluation Information System (Micro-LEIS) has been widely used to assess land suitability around the world [29]. The Micro-LEIS system is based on an integrated soil, climate, and agricultural management databases for assessing land, and contains two models related to land vulnerability and suitability [30]. The Almagra model was designed for land suitability assessment and is one of the major components of Micro-LEIS DSS [31]. The main aim of this work is to use multivariate analysis to assess soil capability in the dryland areas of the northwestern Nile Delta in Egypt. In addition, land suitability for cultivated crops in the study area under CS and OS of soil management was evaluated to determine the most appropriate land use based on physiographic units.

2. Materials and Methods

2.1. The Site Description

The study area was in the northwest Nile Delta in Egypt. It lies between longitudes $30^{\circ}15'0''$ – $30^{\circ}40'0''$ E and latitudes $31^{\circ}7'15''$ – $31^{\circ}30'45''$ N, with a total area of 797.00 km² (Figure 1). The area is categorized by a Mediterranean climate based on the mean climatic parameters for a period of 50.00 years from 1960 to 2011 [32]. A relatively high average maximum temperature of 30 °C is usually recorded during the dry season in August. The mean minimum temperature in January is 13 °C. Precipitation is naturally light and drizzly from November to February, with a mean rainfall of about 17.23 mm/year. The lowest evaporation rates are noticed in January and December owing to low temperatures, while the highest rates are observed in June and September owing to relatively high temperatures.

The annual mean rate of evaporation ranges from 3.3 to 4.8 mm/day. The lowest percentage of relative humidity of 51% is observed in April, while the highest proportion of 58.4% is observed in December. The area has a torric and thermal soil moisture and temperature regime [33]. Geologically, the western Nile Delta is formed from sedimentary deposits that vary in age from the Late Cretaceous to Quaternary. The eastern and western parts of the study area are covered with Holocene clay and Quaternary sediments, respectively [34]. Surface irrigation is the most commonly used system, in which water is pumped from irrigation canals and drained in furrows and basins [18].

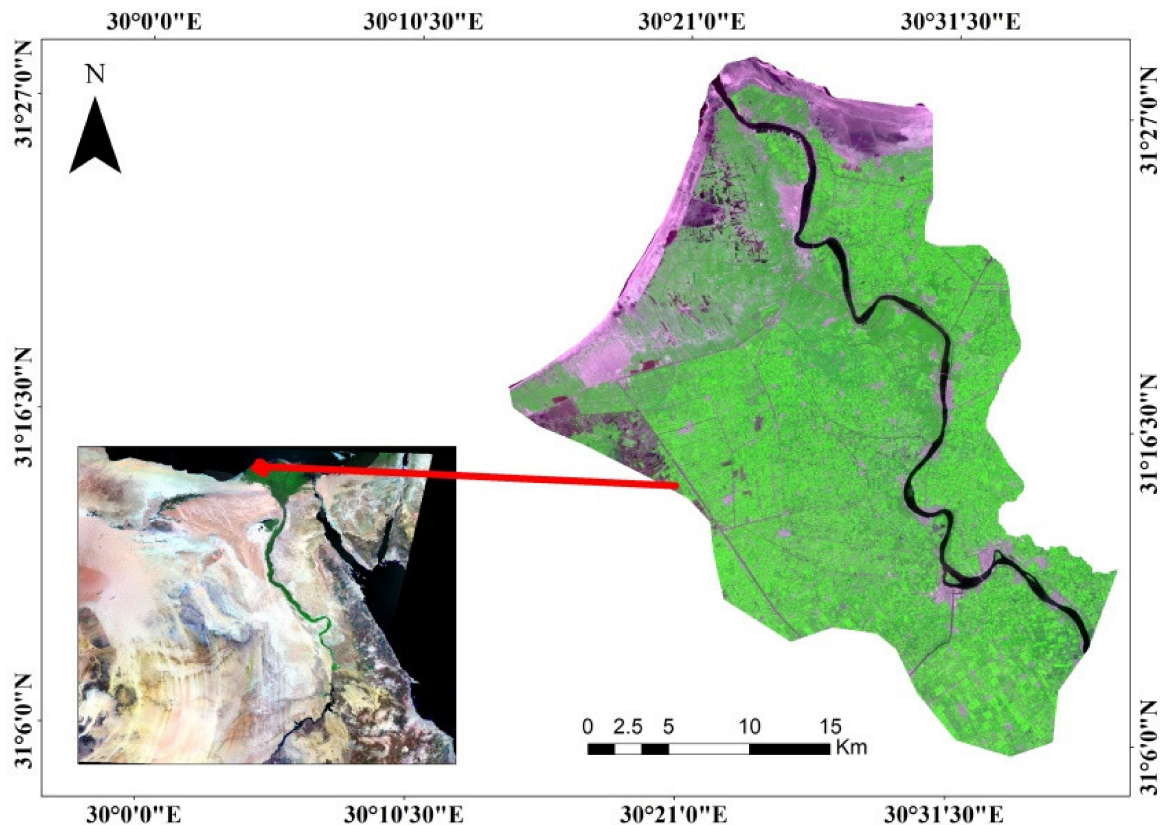


Figure 1. Location of investigated area.

2.2. Extraction of Physiographic Units

In this study, a SENTINEL-2 image acquired in August 2020 under clear-sky conditions was utilized to create landforms and digital soil map features of the study area with the aid of a digital elevation model (DEM). The Sentinel application platform (SNAP) and Environment for Visualizing Images (ENVI 5.4) software were used to process the spectral subset, radiometric calibration, atmospheric, and geometric corrections of the image [35]. Remote sensing (RS) and geographic information system (GIS) are effective for identifying geomorphological units [36]. Thirteen geomorphological units were recognized as representing different geomorphological features within the study area. Subsequently, the image obtained was used as the base map, and each geomorphic unit was homogeneous with the natural land properties [37]. The stepwise methodology for evaluating soil relied on the integrated soil data, remote sensing data, and GIS utilizing multivariate analysis, as illustrated in Figure 2.

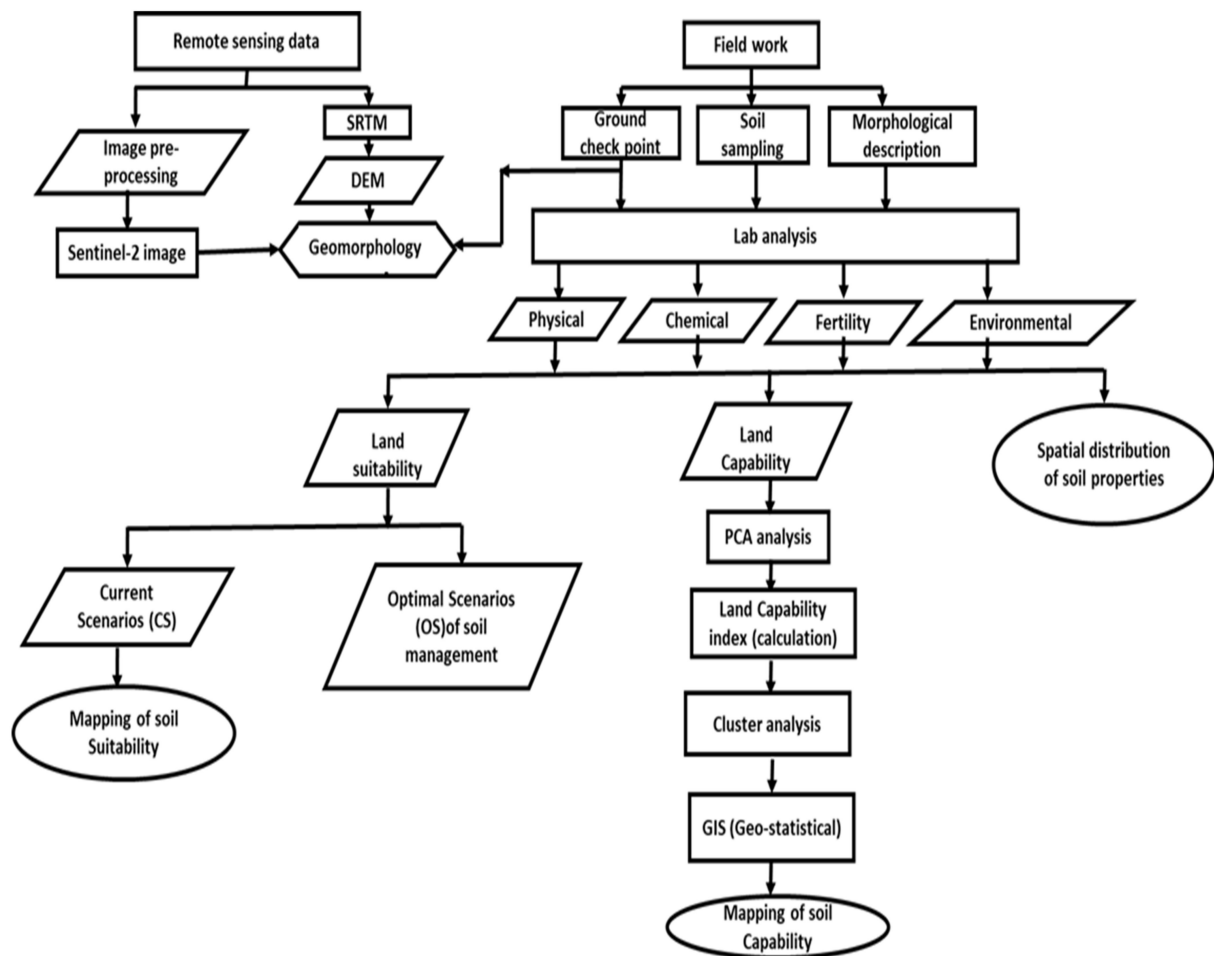


Figure 2. Flow chart illustrating methodology of current work.

2.3. Sample Collection and Lab Analysis

A total of 15 soil profiles were geo-referenced based on geomorphological field mapping of the research area using the Global Positioning System. These profiles were selected from three sampling areas spanning about 80 km² to represent the identified geomorphology and landscape units of the area in Figure 3. Morphological description and classification of soil profiles were carried out according to FAO [12] and USDA [33], respectively. Soil profiles were dug to 150 cm depth or until the water table appeared. Thus, the soil profiles range from 80–150 cm depth. The soil physiochemical parameters (61 soil samples) were analyzed in an ISO/IEC 17025 (2017)-compliant and accredited soil, water, and plant laboratory at the Faculty of Agriculture, Tanta University. Chemical analyses, including salinity (EC), soil reaction (pH), cation exchange capacity (CEC), calcium carbonate percentage (CaCO₃), exchangeable sodium percentage (ESP), and trace elements (As, Co, Cu, Ni, and Zn), were conducted to determine the Irrigation Water Quality Index (IWQI). Trace elements and heavy metals in irrigation water are responsible for soil contamination, and are key indicators of irrigation water quality [38]. In addition, analysis of soil physical characteristics, including bulk density, particle size distribution, and fertility as defined by percentage soil organic matter content (SOM%) and available soil nitrogen (N), phosphorus (P), and potassium (K) was conducted [39–43].

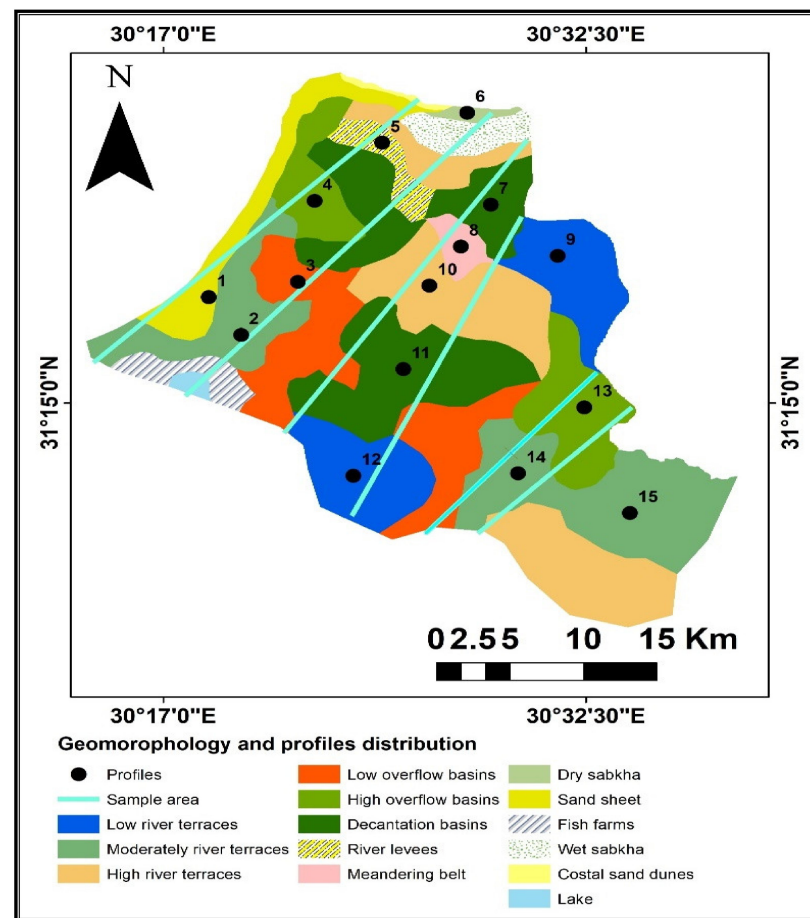


Figure 3. The distribution of soil profiles and sampling areas in this study.

2.4. Determination of IWQI Values

The nature and severity of problems caused by poor irrigation water quality are widely considered to differ based on a variety of factors, such as soil type and crops, the regional environment, and how water is used by farmers. Generally, five measures are used to assess irrigation water quality, including salinity level, infiltration and permeability hazard, and the level of toxic chemicals in water [44,45].

The proposed IWQI, which evaluates the mutual effect of quality parameters, was calculated using Equations (1) and (2):

$$G = \frac{w}{N} \sum_{k=1}^N r_k \quad (1)$$

where k is an incremental index, w is the weight of each hazard, N is the total number of parameters, and r is the rating value of each parameter.

$$IWQ_{\text{index}} = \sum_{i=1}^5 G_i \quad (2)$$

where i is an incremental index and G is the contribution of each water quality parameter, (salinity, infiltration, specific ion toxicity, trace element toxicity, and miscellaneous effects).

2.5. Statistical Analysis

Descriptive statistics of the studied soil characteristics, including the minimum, maximum, arithmetic mean, standard deviation, and coefficient of variation, were computed using SPSS version 25. PCA was used to reduce the dataset into principal component (PC) variables and to avoid multi-collinearity between the original variables. Prior to PCA, the Pearson correlation coefficient was utilized to verify linear relationships among the soil

variables. The Kaiser–Meyer–Olkin (KMO) method was used to assess adequacy of samples for the whole data set, with KMO values larger than 0.5 indicating the suitability of the data for PCA. In addition, data fitness was determined using the Bartlett test, and the results revealed a $p < 0.05$, which further confirmed the data fitness for PCA [46]. SPSS software version 25 was used to perform all statistical analyses. The soil profiles were considered as objects for evaluating soil capability, and were divided into dissimilar clusters utilizing agglomerative hierarchical clustering (AHC) in PCA.

2.6. Soil Capability Assessment Based on PCA

The Weighted Additive method was used according to Equation (3):

$$WAI = \sum_{i=1}^n W_i \times S_i \quad (3)$$

where WAI is the Weighted Additive index, S_i is the score, n is the number of indicators, and W_i is the weight of indicators.

All parameters were weighted based on the communality of indicators, which were computed statistically or obtained using factor analysis (IBM, SPSS Statics 25). The weighted value of each parameter was either calculated by dividing each parameter value by the overall sum of their values or reported as a ratio [47]. Each parameter was analyzed using four indicators, namely, chemical (CI), physical (PI), fertility (FI), and environmental (EI) indices, and scores ranging from 0.2 to 1.0 were obtained (Table S1). The final index values were classified into high capability (C1), moderately high capability (C2), moderate capability (C3), and low capability (C4) categories (Table S2). The range of values for each index was divided by the number of categories obtained (4), and the results were subsequently used as the width of each category. The resulting values were successively added to the lowest values of each index to obtain the upper limits of each category. Soil capability assessment depends on defining soil properties and their relationship with agricultural suitability. In this context, PCA classifies the capability of soil by harmonizing soil properties within each class. In addition, PCA provides a visual representation of the main clustering patterns for identifying similarities and differences among soil characteristics [48].

2.7. Mapping Soil Properties Using Inverse Distance Weighted (IDW)

The IDW tool in ArcGIS10.7 software was used to produce interpolation maps of chemical, fertility, physical, and environment parameters. This approach works by computing the grid note by considering neighboring locations within a user-defined search radius. The IDW is widely used in soil investigations because it is easy to implement [49–54]. The local impact of the measurement point decreases with distance, as illustrated in the following equation:

$$z_p = \frac{\sum_{i=1}^n \left(\frac{z_i}{d_i} \right)}{\sum_{i=1}^n \left(\frac{1}{d_i} \right)} \quad (4)$$

where z_p is the value predicted at point P, z_i is the z value at measured point i, and d_i is the distance between point 0 and point 'i'.

Based on SPSS results, the geometrical interval classification method was used to produce most of the interpolation maps, because these data were not distributed normally, whereas natural breaks classification (Jenks) was used for EC, ESP, and CaCO_3 maps, as the data used for these maps were normally distributed.

2.8. Determination of Land Suitability

The Almagra model defines soil suitability in five different clusters, namely, optimum (S1), high (S2), moderate (S3), marginal (S4), and unsuitable (S5), for five traditional annual crops, including wheat, maize, and potato, as well as for semiannual and perennial crops such as alfalfa and citrus, respectively. The model was implemented in Micro-LEIS and uses soil variables and favorable crop conditions to evaluate suitability [29,31,55]. The

variable generalization levels were determined based on crop requirements for each soil parameter using the most limiting factor method to define soil suitability classes. In this study, the Almagra model was implemented to assess the CS of soil suitability for five crops that are predominantly cultivated within the study area. The OS was based on manageable soil parameters, such as EC, ESP, and CaCO₃, without considering the interaction between them. Other soil parameters such as texture and depth were not considered owing to the difficulty in their modification.

The suggested OS was calculated based on Equation (5) [30]:

$$OS = CS - UR_s \quad (5)$$

where OS, CS, and URs represent the optimal scenario, the current scenario, and the units of reduction, respectively.

The reduction units were defined by assessing CS to meet the suggested fixed value of OS to raise the final soil suitability class. Notably, when the soil under CS was unsuitable (S5) or marginally suitable (S4), higher URs were required relative to those of moderate suitability (S3), which required lower URs to meet the fixed OS value for each soil variable. Under OS, EC classes were reduced and the values varied from slightly to highly saline, with a fixed value of 2 dSm⁻¹, which represents nonsaline soil. For ESP, the projected value of OS was 5%. Finally, OS decreased the CaCO₃ values from 9.04% to <2.

3. Results and Discussion

3.1. Geomorphology of the Study Area

The geomorphological units of the study area were determined using Sentinel-2 satellite imagery, DEM, and field truth points (Figure 4). The study area included flood plain, lacustrine plain, and marine plain as the three main landscape features. These features are very common in the north of the Nile Delta and the southern areas of lakes such as Idku in Egypt [1,56]. The flood plain (713 km²) formed from deposits of the Nile before the high dam's construction. There are many landforms under this landscape, i.e., river terraces, overflow basins, decantation basins, river levees, and meandering belt. The lacustrine plain (40 km²) is formed from Holocene-era lacustrine sediments. This landscape includes fish farms, dry and wet sabkha, and coastal sand dunes. The marine plain (40 km²) is located in the north zone of the study area, and includes sand sheet landforms. Water bodies (Lakes) represent 4 km² of the total area.

3.2. Spatial Analysis and Soil Physiochemical Properties

3.2.1. Chemical and Physical Soil Capability Indicators

Chemical soil capability indicators (CSCI) are dynamic indicators that vary over time as a result of land management. The CSCI were chosen based on their sensitivity to disturbance and their ability to execute soil ecosystem functions. CSCI included EC, pH, ESP, CaCO₃, and CEC as well as physical indicators including depth, as represented in Figure S1.

The spatial trends of EC and ESP increased in the upper part of the northwest of the study area (around 12–20 dS/m and 18–25%), respectively. The high values of ECE in certain areas of the study area may have resulted from the high salinity of the water table and the effects of lake water and seawater. This agrees with the common pattern of the northern delta, where most of the soil is categorized by high soil salinity [15,57]. This high sodium percentage can negatively affect soil properties such as soil structure and hydrology, consequently reducing crop productivity [7]. The highest values of pH (approximately 8.6–8.9) were found in sites in the northeast and southeast of the study area. The highest values of CaCO₃ (roughly 6–9%) were found in the middle and southwest of the studied area due to shell fragments, which can lead to solid layer formations impermeable to crops of plants and water in addition to fixation of P fertilizer [7,58]. From the interpolation map, the highest value of CEC (around 37–42 cmolc/kg) was found in sites in southwest and middle of study area. The profile depth ranged from 80–150 cm.

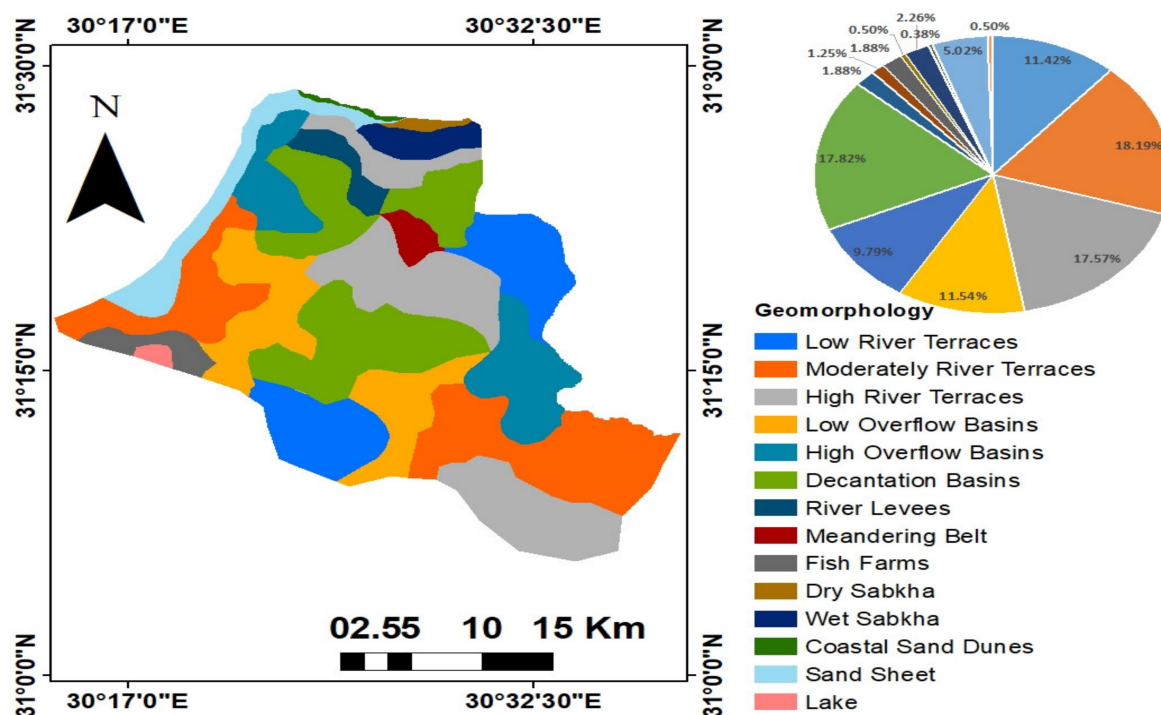


Figure 4. Geomorphological map illustrating the study area.

3.2.2. Fertility and Environmental Soil Capability Indicators

The spatial distribution map for available N, P, K, and SOM in Figure S2 shows that the trend of both N, with values ranging from 7.50 to 81 mg/kg, and P, with values ranging from 6.30 to 22.3 mg/kg, increased from north to south across the study area. On the other hand, the spatial trend of K, with values ranging from 9.30–457.1 mg/kg, increased in sites in the upper north and lower south of the study area. The highest values of SOM (0.9–1.22%) were found in the middle of the northeast and northwest of the study area. The IWQI map (Figure S3) is thought to be a useful tool in future agricultural management plans [18].

3.3. Multivariate Statistical Analysis

3.3.1. Descriptive Statistics of Soil Indicators

Fifteen soil characteristics were analyzed as prospective soil capability indicators. The descriptive statistics obtained based on the weighted mean of parameters of investigated soil profiles are provided in Table S3. The skewness and kurtosis of the tested soil properties revealed a normal distribution in EC, ESP, and CaCO_3 , while other properties had skewed distribution. The normality test using the Anderson–Darling method obtained p values < 0.05 for all the tested soil properties.

3.3.2. Correlations of Soil Physicochemical Indicators and Principal Component Analysis

The Pearson correlation coefficient plot revealed both positive and negative coefficients at both $p < 0.01$ or $p < 0.05$ (Figure 5). A significant positive association was observed between depth and both EC and ESP, with $r = 0.38$ and 0.41 , respectively. Similarly, significant positive coefficients of $r = 0.55$, 0.56 , 0.57 , 0.5 , and 0.34 were observed between depth and AK, AN, AP, CEC, and OM, respectively. In addition, positive significant correlations of $r = 0.87$ between EC and ESP and 0.46 between EC and AP were detected. In contrast, negative correlation coefficients were observed between pH and other properties, except for ESP and CaCO_3 . Notably, higher positive correlations were observed between OM and CaCO_3 , AN, AP, AK, and CEC, with coefficients of $r = 0.48$, 0.80 , 0.71 , 0.82 , and 0.89 , respectively. In addition, a positive significant correlation between CEC and AN ($r = 0.94$), AP ($r = 0.84$), and AK ($r = 0.95$) was observed.

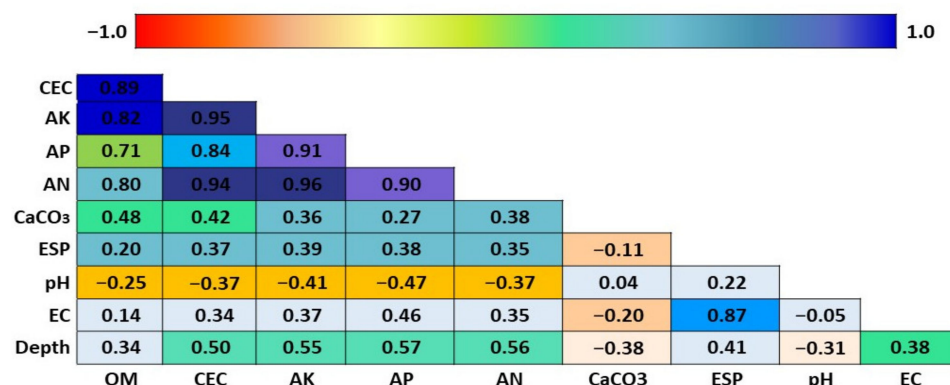


Figure 5. Correlation plot showing coefficients between soil properties. Note: $p < 0.01$ and/or $p < 0.05$. AK, AP, and AN represent available potassium, phosphorus, and nitrogen, respectively.

The factor loading results revealed the acceptable clustering of soil properties and confirmed the reliability of PCA for defining soil characteristics in different clusters [59]. PCA was used to assess land capability based on the variation in soil physicochemical properties and environmental conditions. The method uses eigenvalues, proportions of variance, and cumulative variance of PCs to estimate clusters based on soil characteristics. In this study, PCs with eigenvalues > 1 were retained, while those with values < 1 were screened out. As a result, the first four groups with eigenvalues > 1 were selected. The soil indicators and these four PCs are shown in Table 1. Notably, a cumulative variance of 91.24% for all the tested variables was observed, with PC1, PC2, PC3, and PC4 explaining about 51.12%, 18.37%, 12.48%, and 9.27% of the total variance, respectively. The factor loadings and component score coefficient outputs from the varimax method showed higher factor loads. The most representative physical and chemical indicators for PC1 based on their close correlation included AN, AP, AK, OM, CEC, and CaCO_3 , which might be due to the association between natural conditions and the soil formation processes in the study area [60]. In contrast, PC2 was correlated with soil depth, pH, and IWQI. In addition, PC3 was linked with EC and ESP, while PC4 was attributed to ESP.

Table 1. Summary of PCA.

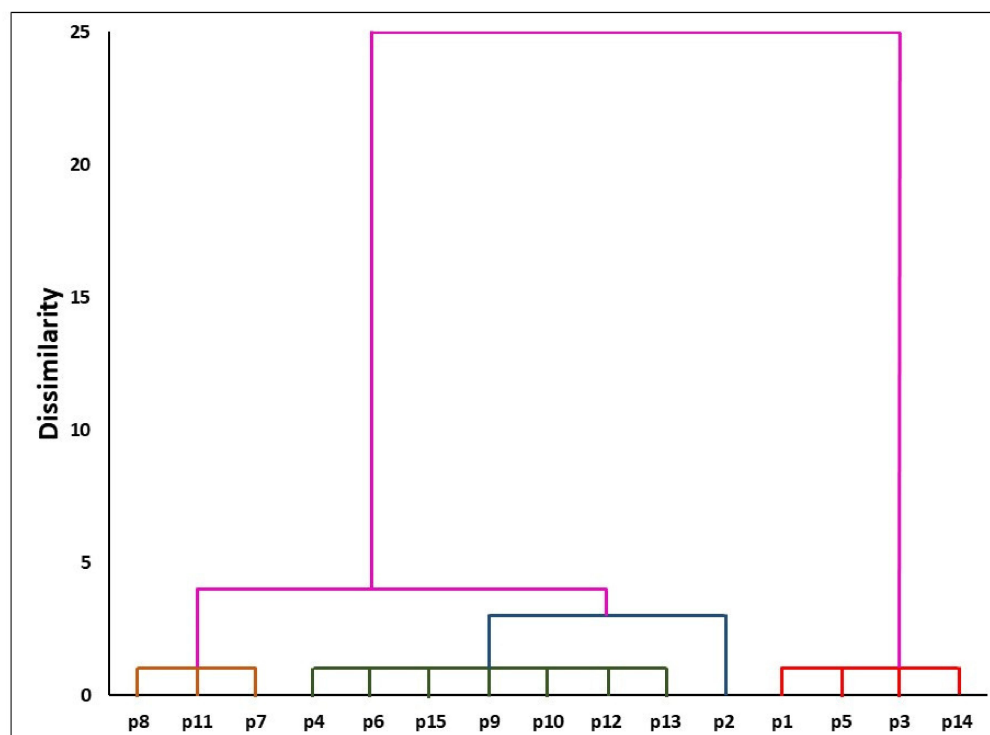
PC Parameters	PC1	PC2	PC3	PC4
Eigenvalue	5.62	2.02	1.37	1.02
Variability (%)	51.12	18.37	12.48	9.27
Cumulative (%)	51.12	69.49	81.96	91.24
Component score coefficients				
Indicator	PC1	PC2	PC3	PC4
Depth	0.64	0.47	-0.44	0.04
EC (dSm^{-1})	0.49	0.70	0.36	-0.24
pH	-0.41	0.20	0.60	0.58
ESP	0.48	0.69	0.51	0.02
CaCO_3	0.28	-0.76	0.52	0.06
AN	0.96	-0.15	0.02	-0.01
AP	0.93	-0.05	-0.00	-0.23
AK	0.97	-0.13	0.04	-0.07
CEC	0.96	-0.17	0.04	0.10
OM	0.83	-0.34	0.06	0.24
IWQI	0.42	0.20	-0.41	0.71

Table 2 shows the acceptable level of p values for the Bartlett sphericity and the KMO tests at $p = 0.05$. The Bartlett sphericity test revealed a p value of < 0.0001 , which confirmed the suitability of PCA for defining soil clusters based on their characteristics.

Table 2. The Kaiser–Meyer–Olkin (KMO) and Bartlett sphericity tests.

KMO and Bartlett Tests		
KMO Measure of Sampling Adequacy		0.692
Bartlett Test of Sphericity	Chi-square (approx. value)	138.160
	Degree of freedom (DF)	55
	<i>p</i> value	0.0001

The cluster analysis revealed two dissimilar clusters based on PC scores. A dendrogram showing hierarchical clustering of the four groups based on soil properties was obtained, with each group sharing soil profiles that contained a set of similar characteristics (Figure 6).

**Figure 6.** Agglomerative hierarchical clustering dendrogram showing clustering based on soil properties.

3.3.3. Assessment of Land Capability Based on PCA

Soil characteristics classification and its correlation with soil capability and crop suitability is an unprecedented soil analysis approach that can overcome the challenge of classifying soils into clusters based on similarities in their properties, which relies on the intricate determination of increasing and decreasing soil characteristics. The investigated area land capability map was constructed using PCA results; the map reflected the four previously identified groups (Figure 7). The statistical analysis of soil parameters for land capability clusters (C1–C4) are shown in (Table 3). The high capability cluster (C1) occupied 31.83% of the total investigated area, with the soils of this class being identified by moderate salinity, ESP, IWQI, and CaCO₃ values. The moderately high capability class (C2) accounted for 37.88% of the total study area. The limiting factors of this class were high CaCO₃ content of 9.04% and shallow soil depth of 80 cm. The moderate capability class (C3) accounted for 28.27% of the total study area, and the unit was characterized by a number of limitations, such as high pH and salinity values, which represented the major limiting factors for soil capability, and low SOM%. In addition, the soils of C3 showed a moderate ESP content of 14.01%. The low capability class (C4) represented a small area of 2.02% of the total study area. The soil chemical analysis of this class illustrated high salinity values and moderate ESP and SOM contents.

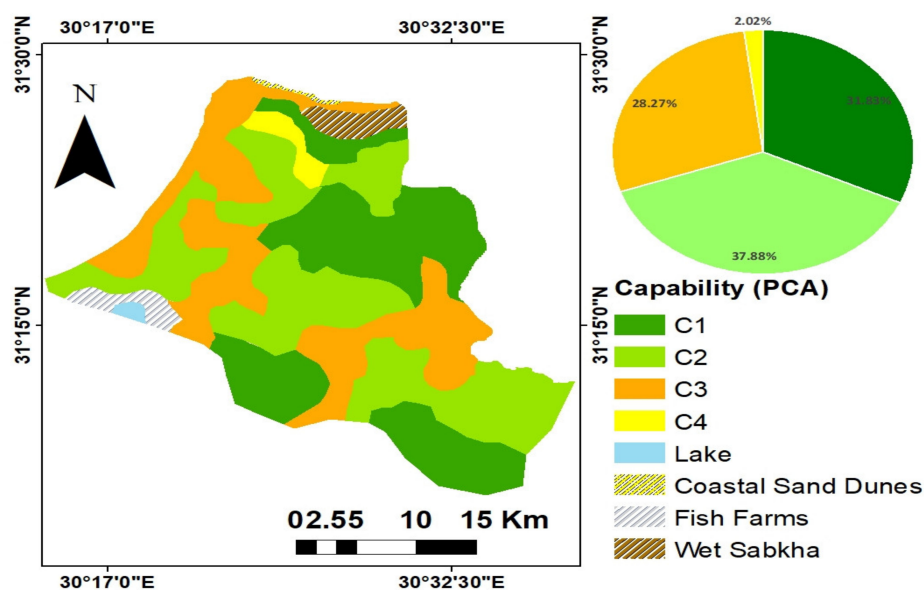


Figure 7. Land capability classes within study area.

Table 3. Statistical summary of soil properties in the four land capability clusters.

Classes	Depth	EC (dS/m)	pH	ESP	CaCO ₃	AN	AP	AK	CEC	OM	IWQI
C1	108	2.22	8.58	7.01	2.80	13.55	8.43	14.18	9.34	0.38	30.67
C2	80	1.50	8.37	4.73	9.04	63.00	17.40	413.30	36.84	1.17	26.50
C3	123	5.32	8.67	12.76	3.97	43.60	12.53	272.13	32.26	0.93	37.40
C4	150	7.92	8.37	14.01	3.77	68.16	19.41	409.80	39.42	0.97	34.28

3.3.4. Soil Suitability

Soil profiles were evaluated based on their suitability for crop production by considering the specific soil property requirements of each crop to achieve maximum yield. The results showed that soil suitability of selected crops could be categorized into S2–S5 classes, with different limiting factors being identified in each class based on geomorphological units. The soil suitability was examined with five horticultural and field crops, namely, wheat, maize, alfalfa, potato, and citrus (Figure 8). Overall, cultivating field crops in the area demonstrated good potential for sustainable agricultural development (Figure S4); however, improved quality of irrigation water is highly necessary [18].

3.3.5. Soil Factors under Current and Optimal Scenarios

The key soil limiting factors in the study area were identified to be high salinity, increased sodium saturation, poor drainage, calcium carbonate, and rough soil texture (Figures S5 and S6). Reducing the manageable soil limiting severity of factors, such as EC, ESP, CaCO₃, and drainage, where possible, resulted in enhanced soil suitability for all selected crops under OS. In addition, under OS, soils in all suitability classes showed decreased salinity contents to 2 dSm⁻¹, which correspond to non-saline soil levels. No detectable change in salinity content was observed in nonsaline soil (<2 dSm⁻¹), while 10–18 reduction units were observed in highest-salinity soils with contents of 12–20 dSm⁻¹. Numerous soil management options have been proposed to decrease soil salinity, such as using low-salinity water to enhance the leaching of salts from the soil root zone [61]. The rate of plant growth under salt stress strongly varies among plant species [62,63]. Sodium saturation values can be reduced to low sodium levels of 5% with 4–20 reduction units. Previous studies have demonstrated that the addition of gypsum can lower high soil sodium saturation content [64–66] owing to its ability to absorb calcium instead of sodium in soil particles, directly leading to improved aggregation and decreased pH [65,67].

In addition, low values of SOM may affect the soil structure negatively [68]. Thus, it is recommended to raise the SOM level by adding organic amendments and residues of crops such as leguminous plants [69]. Similarly, about 1.6–7 reduction units are necessary to improve calcium carbonate content to the optimum <2% level. The best practice in the study area is to cultivate different seasonal crops and to avoid replanting the same plants in the same sites in order to maintain soil fertility and increase the SOM level [68–76]. This helps to maintain soil quality over the long run, which leads to an increased degree of crop yield and soil sustainability for different varieties of crops [68]. The spatial distribution of salinity, sodium saturation, and calcium carbonate under CS and their projected reduction units in each suitability class are shown in Figure 9. The status of the agricultural drainage system in the investigated area ranged from excessive to poor (Figure S6) and was predominantly poor under CS.

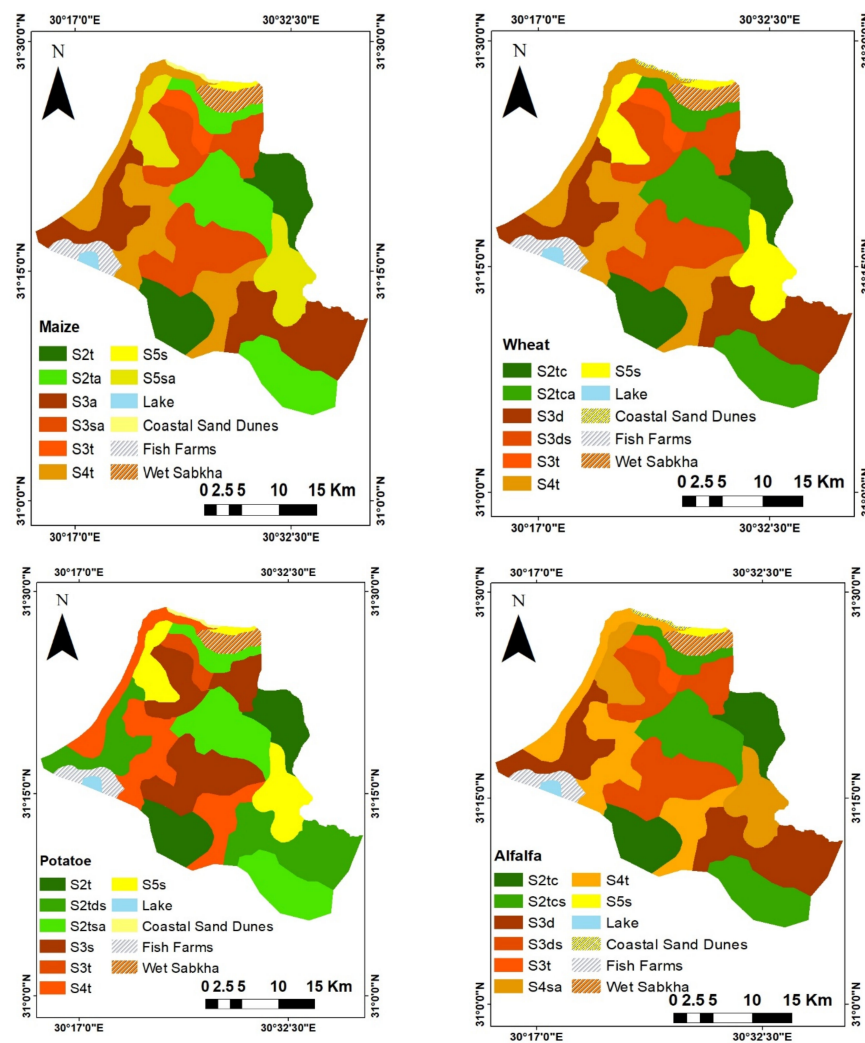


Figure 8. Cont.

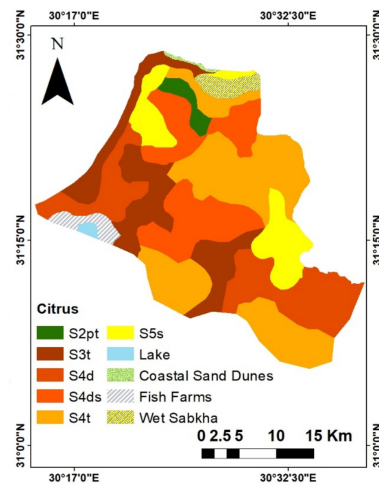


Figure 8. Maps showing soil suitability classes (S1–S5) for selected field and horticultural crops. Lowercase letters represent main soil limiting factors in each class; s, salinity; t, texture; a, sodium saturation; d, drainage; c, carbonate content; p, profile depth.

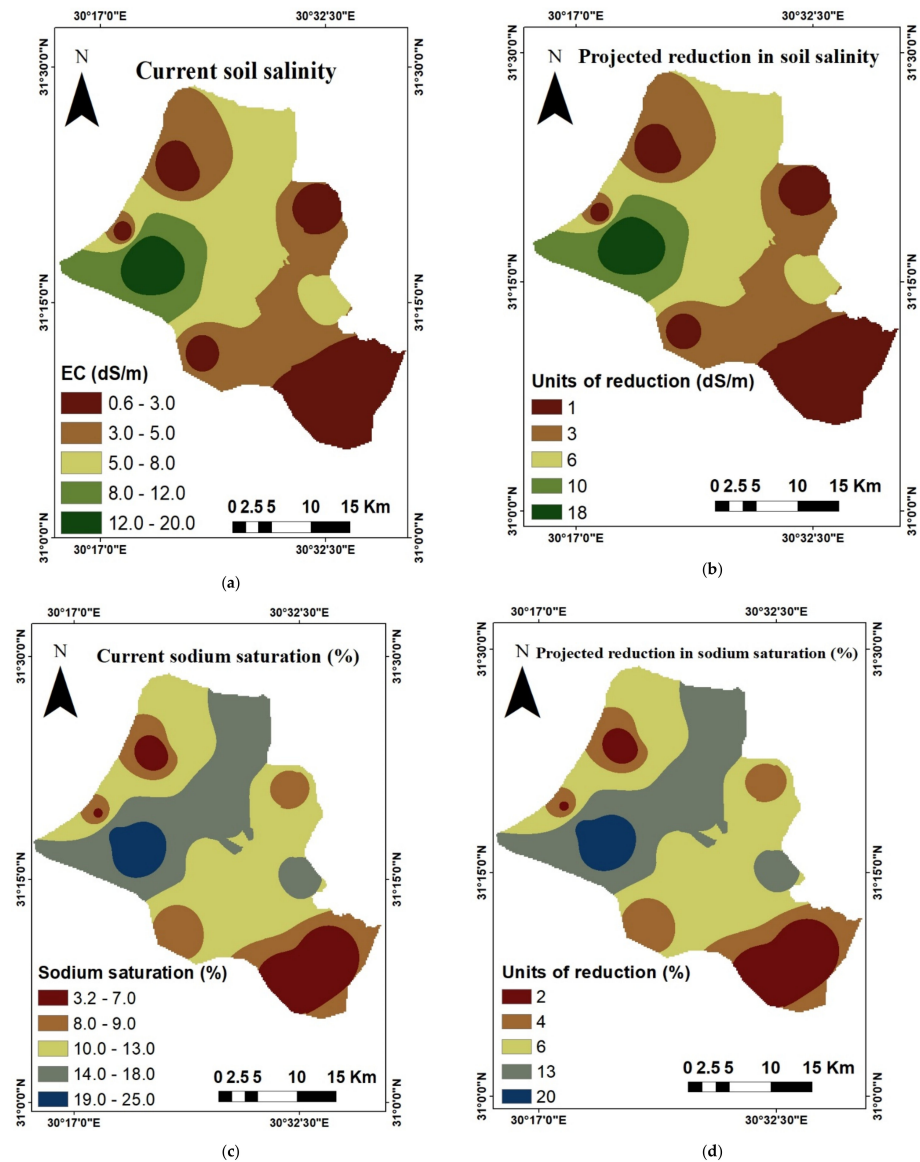


Figure 9. Cont.

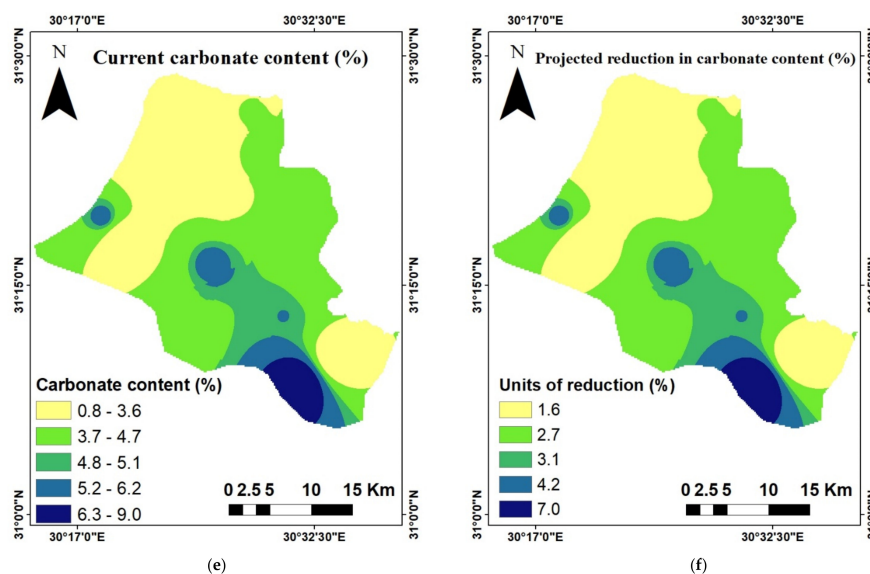


Figure 9. Spatial distribution of soil factors under CS and their projected reduction units under OS: soil salinity (a,b), sodium saturation (c,d), and carbonate content (e,f).

3.3.6. Evaluation of Soil Suitability under CS and OS

Geomorphic features such as coastal sand dunes, wet sabkha, and fish farms, which cumulatively account for 4.52% of the total study area, were not considered in the suitability evaluation. In addition, water bodies (lakes), which account for 0.5% of the total study area, were not considered in the suitability evaluation. Under CS, subclasses 8–20 represented the main soil suitability subclasses, covering suitability classes S2, S3, S4, and S5 for most evaluated crops (Figure 8). With the application of OS, the moderate suitability class (S3) and the unsuitable class (S5) were enhanced to the suitable (S2) and marginally suitable (S4) classes, respectively, while the high suitability class (S1) showed increased area, which had significant effects on the suitability of maize crop (Table 4).

Table 4. The soil suitability for the five crops evaluated.

Class	Crops									
	Wheat		Maize		Potato		Alfalfa		Citrus	
	A	B	A	B	A	B	A	B	A	B
S1	–	–	–	39.9	–	–	–	–	–	–
S2	31.8	82.6	31.8	42.7	51.0	82.6	31.8	82.6	2.0	39.9
S3	39.9	–	39.9	–	20.7	–	39.9	–	17.4	17.4
S4	17.4	17.4	17.4	17.4	17.4	17.4	27.8	17.4	69.7	42.7
S5	10.9	–	10.9	–	10.9	–	0.5	–	10.9	–
Total	100	100	100	100	100	100	100	100	100	100

Note: (A) Current situation and (B) optimal scenario.

4. Conclusions

Integrated PCA and AHC analysis were used to classify soil capability within the study area, relying on the associations and interactions between soil characteristics. The study area could be classified into four classes relying on PCA. The main limiting factors within the study area included shallow depth, high salinity, and high CaCO₃ content in certain sites. Subsequently, multivariate analysis was used to assess soil capability based on its properties under different conditions. The observed crop suitability under CS can provide valuable information to decision-makers about key limiting factors. Moreover, evaluation of crop suitability under OS could potentially be used to predict the degree of improvements necessary to achieve agricultural sustainability. Similarly, remote sensing

data are useful for extracting geomorphologic units, which are considered the base map for soil evaluation studies. GIS techniques are vital tools for mapping soil capability and crop suitability in order to achieve the best land use and food security in arid zones.

Supplementary Materials: The following supporting information can be downloaded at: <https://www.mdpi.com/article/10.3390/land11071027/s1>, Figure S1: Spatial distribution of chemical and physical soil properties: (a) electric conductivity (EC: dS/m), (b) soil reaction (pH), (c) exchangeable sodium percent (ESP), (d) calcium carbonate percentage (CaCO₃: %), (e) cation exchange capacity (CEC: cmolc/Kg), and (f) depth (cm); Figure S2: Spatial distribution of fertility soil properties: (a) (Available N: mg/kg), (b) (Available P: mg/kg), (c) (Available K: mg/kg), (d) Soil Organic Matter (SOM %); Figure S3: The IWQ index map of the study area Figure S4: Cultivated orchards (a) Mango and (b) Orange in the study area; Figure S5: Saline soils near the fish ponds south of Idku lake in the studied area; Figure S6: Very poorly drained soil in the study area; Table S1: Scores of all parameters; Table S2: Final SC range of study area; Table S3: Statistical characterization of the weighted mean of the studied soil profiles properties ($n = 61$).

Author Contributions: Conceptualization, R.A.E.B. and M.S.S. methodology, M.S.S.; software, R.A.E.B. and M.S.S.; validation R.A.E.B. and M.S.S.; formal analysis, R.A.E.B. and M.S.S.; investigation, M.S.S.; resources R.A.E.B. and M.S.S.; data curation, R.A.E.B., A.A.E.B., M.M.I. and M.S.S.; writing—original draft preparation, R.A.E.B.; writing—review and editing, A.A.E.B., M.M.I., E.S.M. and D.E.K.; visualization, A.A.E.B., M.M.I. and M.S.S.; supervision, A.A.E.B., M.M.I. and M.S.S.; project administration, A.A.E.B. and M.M.I.; funding acquisition, E.S.M. and D.E.K. All authors have read and agreed to the published version of the manuscript.

Funding: This research received no external funding.

Data Availability Statement: Not applicable.

Acknowledgments: This paper was supported by the RUDN University Strategic Academic Leadership Program.

Conflicts of Interest: The authors declare no conflict of interest.

References

- Baroudy, A.A.; Ali, A.M.; Mohamed, E.S.; Moghanm, F.S.; Shokr, M.S.; Savin, I.; Poddubsky, A.; Ding, Z.; Kheir, A.M.S.; Aldosari, A.A.; et al. Modeling land suitability for rice crop using remote sensing and soil quality indicators: The case study of the Nile Delta. *Sustainability* **2020**, *12*, 9653. [[CrossRef](#)]
- Tahmasebinia, F.; Tsumura, Y.; Wang, B.; Wen, Y.; Bao, C.; Sepasgozar, S.; Alonso-Marroquin, F. Floating Cities Bridge in 2050. In *Smart Cities and Construction Technologies*; IntechOpen: London, UK, 2020.
- Debiagi, F.; Madeira, T.B.; Nixdorf, S.L.; Mali, S. Pretreatment efficiency using autoclave high-pressure steam and ultrasonication in sugar production from liquid hydrolysates and access to the residual solid fractions of wheat bran and oat hulls. *Appl. Biochem. Biotechnol.* **2020**, *190*, 166–181. [[CrossRef](#)] [[PubMed](#)]
- Xiang, T.; Malik, T.H.; Nielsen, K. The impact of population pressure on global fertilizer use intensity, 1970–2011: An analysis of policy-induced mediation. *Technol. Forecast. Soc.* **2020**, *152*, 119895. [[CrossRef](#)]
- Gerten, D.; Heck, V.; Jägermeyr, J.; Bodirsky, B.L.; Fetzer, I.; Jalava, M.; Kummu, M.; Lucht, W.; Rockström, J.; Schapho, S.; et al. Feeding ten billion people is possible within four terrestrial planetary boundaries. *Nat. Sustain.* **2020**, *3*, 200–208. [[CrossRef](#)]
- Tir, J.; Diehl, P.F. Demographic Pressure and Interstate Conflict. In *Environmental Conflict*; Routledge: London, UK, 2018; pp. 58–83.
- Shokr, M.S.; Abdellatif, M.A.; El Baroudy, A.A.; Elnashar, A.; Ali, E.F.; Belal, A.A.; Attia, W.; Ahmed, M.; Aldosari, A.A.; Szantoi, Z.; et al. Development of a Spatial Model for Soil Quality Assessment under Arid and Semi-Arid Conditions. *Sustainability* **2021**, *13*, 2893. [[CrossRef](#)]
- Bakr, N.; Bahnassy, M.H. *Egyptian Natural Resources: In the Soils of Egypt*; Springer: Cham, Switzerland, 2019; pp. 33–49.
- Satoh, M.; Aboulroos, S. *Irrigated Agriculture in Egypt: Past, Present and Future*; Springer: Cham, Switzerland, 2017.
- Abd-Elmabod, S.K.; Fitch, A.C.; Zhang, Z.; Ali, R.R.; Jones, L. Rapid urbanisation threatens fertile agricultural land and soil carbon in the Nile Delta. *J. Environ. Manag.* **2019**, *252*, 109668. [[CrossRef](#)]
- Saleh, A.M.; Belal, A.B.; Mohamed, E.S. Land resources assessment of El-Galaba basin, South Egypt for the potentiality of agriculture expansion using remote sensing and GIS techniques. *Egypt. J. Remote Sens. Space Sci.* **2015**, *18*, S19–S30. [[CrossRef](#)]
- Food and Agriculture Organization of the United Nations. *Guidelines for Soil Profile Description*, 3rd ed.; Food and Agriculture Organization of the United Nations: Rome, Italy, 2006.
- Mandal, S.; Choudhury, B.U.; Satpati, L. Soil site suitability analysis using geo-statistical and visualization techniques for selected winter crops in Sagar Island, India. *Appl. Geogr.* **2020**, *122*, 102249. [[CrossRef](#)]

14. Abdelrahman, M.A.E.; Shalaby, A.; Mohamed, E.S. Comparison of two soil quality indices using two methods based on geographic information system. *Egypt. J. Remote Sens. Space Sci.* **2019**, *22*, 127–136. [[CrossRef](#)]
15. Hammam, A.A.; Mohamed, E.S. Mapping soil salinity in the East Nile Delta using several methodological approaches of salinity assessment. *Egypt. J. Remote Sens. Space Sci.* **2020**, *23*, 125–131. [[CrossRef](#)]
16. Hassan, A.M.; Belal, A.A.; Hassan, M.A.; Farag, F.M.; Mohamed, E.S. Potential of thermal remote sensing techniques in monitoring waterlogged area based on surface soil moisture retrieval. *J. Afr. Earth Sci.* **2019**, *155*, 64–74. [[CrossRef](#)]
17. Elbeih, S.F.; El-Zeiny, A.M. Qualitative assessment of groundwater quality based on land use spectral retrieved indices: Case study Sohag Governorate, Egypt. *Remote Sens. Appl. Soc. Environ.* **2018**, *10*, 82–92. [[CrossRef](#)]
18. El Behairy, R.A.; El Baroudy, A.A.; Ibrahim, M.M.; Kheir, A.M.S.; Shokr, M.S. Modelling and assessment of irrigation water quality index using GIS in semi-arid region for sustainable agriculture. *Water Air Soil Pollut.* **2021**, 232–352. [[CrossRef](#)]
19. Mohamed, E.S.; Baroudy, A.A.E.; El-beshbeshy, T.; Emam, M.; Belal, A.A.; Elfadaly, A.; Aldosari, A.A.; Ali, A.M.; Lasaponara, R. Vis-NIR Spectroscopy and Satellite Landsat-8 OLI Data to Map Soil Nutrients in Arid Conditions: A Case Study of the Northwest Coast of Egypt. *Remote Sens.* **2020**, *12*, 3716. [[CrossRef](#)]
20. Burrough, P.A.; McDonnell, R.; McDonnell, R.A.; Lloyd, C.D. *Principles of Geographical Information Systems*; Oxford University Press: Oxford, UK, 2015.
21. Shokr, M.S.; El Baroudy, A.A.; Fullen, M.A.; El-beshbeshy, T.R.; Ali, R.R.; Elhalim, A.; Guerra, A.J.T.; Jorge, M.C.O. Mapping of heavy metal contamination in alluvial soils of the Middle Nile Delta of Egypt. *J. Environ. Eng. Landsc. Manag.* **2016**, *24*, 218–231. [[CrossRef](#)]
22. Abd-Elmabod, S.K.; Mansour, H.M.; Hussein, A.A.; Zhang, Z.; Anaya-Romero, M.; de la Rosa, D.; Jordán, A. Influence of Irrigation Water Quantity on the Land Capability Classification. *Plant Arch.* **2019**, *19*, 2253–2261.
23. Belal, A.A.; Mohamed, E.S.; Abu-Hashim, M.S.D. Land evaluation based on GIS-spatial multi-criteria evaluation (SMCE) for agricultural development in dry Wadi, Eastern Desert. *Egypt. Int. J. Soil Sci.* **2015**, *10*, 100–116. [[CrossRef](#)]
24. Mohamed, E.S.; Ali, A.; El-Shirbeny, M.; Abutaleb, K.; Shaddad, S.M. Mapping soil moisture and their correlation with crop pattern using remotely sensed data in arid region. *Egypt. J. Remote Sens. Space Sci.* **2019**, *23*, 347–353. [[CrossRef](#)]
25. Mohamed, E.S.; Saleh, A.M.; Belal, A.B.; Gad, A. Application of near-infrared reflectance for quantitative assessment of soil properties. *Egypt. J. Remote Sens. Space Sci.* **2018**, *21*, 1–14. [[CrossRef](#)]
26. Csomós, E.; Héberger, K.; Simon-Sarkadi, L. Principal component analysis of biogenic amines and polyphenols in Hungarian wines. *J. Agric. Food Chem.* **2002**, *50*, 3768–3774. [[CrossRef](#)]
27. Muñoz-Rojas, M.; Doro, L.; Ledda, L.; Francaviglia, R. Application of CarboSOIL model to predict the effects of climate change on soil organic carbon stocks in agro-silvo-pastoral Mediterranean management systems. *Agric. Ecosyst. Environ.* **2015**, *202*, 8–16. [[CrossRef](#)]
28. Muñoz-Rojas, M.; Abd-Elmabod, S.K.; Zavala, L.M.; De la Rosa, D.; Jordán, A. Climate change impacts on soil organic carbon stocks of Mediterranean agricultural areas: A case study in Northern Egypt. *Agric. Ecosyst. Environ.* **2017**, *238*, 142–152. [[CrossRef](#)]
29. De la Rosa, D.; Mayol, F.; Diaz-Pereira, E.; Fernandez, M. A land evaluation decision support system (MicroLEIS DSS) for agricultural soil protection. *Environ. Modell. Softw.* **2004**, *19*, 929–942. [[CrossRef](#)]
30. Abd-Elmabod, S.K.; Bakr, N.; Muñoz-Rojas, M.; Pereira, P.; Zhang, Z.; Cerdà, A.; Jordán, A.; Mansour, H.; De la Rosa, D.; Jones, L. Assessment of soil suitability for improvement of soil factors and agricultural management. *Sustainability* **2019**, *11*, 1588. [[CrossRef](#)]
31. Abd-Elmabod, S.K.; Jordán, A.; Fleskens, L.; Phillips, J.D.; Muñoz-Rojas, M.; Van der Ploeg, M.; Anaya-Romero, M.; De la Rosa, D. Modelling agricultural suitability along soil transects under current conditions and improved scenario of soil factors. In *Soil Mapping and Process Modeling for Sustainable Land Use Management*; Elsevier: Amsterdam, The Netherlands, 2017; pp. 193–219. [[CrossRef](#)]
32. Climatological Normal for Egypt. *The Normal for Beheira Governorate from 1960–2011*; Ministry of Civil Aviation, Meteorological Authority: Cairo, Egypt, 2011.
33. Soil Survey Staff. *Keys to Soil Taxonomy, USDA-NRCS*, 11th ed.; U.S. Government Print Office: Washington, DC, USA, 2014.
34. Dawoud, M.A.; Darwish, M.M.; El-Kady, M.M. GIS-based groundwater management model for Western Nile Delta. *Water Resour. Manag.* **2005**, *19*, 585–604. [[CrossRef](#)]
35. El Behairy, R.A. Using New Techniques for Studying Land Resources in Some Areas of North West Nile Delta, Egypt. Master's Thesis, Faculty of Agriculture, Tanta University, Cairo, Egypt, 2021.
36. Said, M.E.S.; Ali, A.M.; Borin, M.; Abd-Elmabod, S.K.; Aldosari, A.A.; Khalil, M.M.N.; Abdel-Fattah, M.K. On the use of multivariate analysis and land evaluation for potential agricultural development of the Northwestern Coast of Egypt. *Agronomy* **2020**, *10*, 1318. [[CrossRef](#)]
37. El Baroudy, A.A. Geomatics-based soil mapping and degradation risk assessment of Nile delta soils. *Pol. J. Environ. Stud.* **2010**, *1123*, 1131.
38. Antoniadis, V.; Shaheen, S.M.; Levizou, E.; Shahid, M.; Niazi, N.K.; Vithanage, M.; Ok, Y.S.; Bolan, N.; Rinklebe, J. A critical prospective analysis of the potential toxicity of trace element regulation limits in soils worldwide: Are they protective concerning health risk assessment?—A review. *Environ. Int.* **2019**, *127*, 819–847. [[CrossRef](#)] [[PubMed](#)]
39. Rhoades, J.D. Salinity: Electrical Conductivity and Total Dissolved Solids. In *Methods of Soil Analysis Part 3, Chemical Methods*; Sparks, D.L., Ed.; Soil Science Society of America Book Series, No. 5; Soil Science Society of America, American Society of Agronomy: Madison, WI, USA, 1996; pp. 417–435.

40. Thomas, G.W. Soil pH and Soil Acidity. In *Methods of Soil Analysis Part 3, Chemical Methods*; Sparks, D.L., Ed.; Soil Science Society of America Book Series, No. 5; Soil Science Society of America, American Society of Agronomy: Madison, WI, USA, 1996; pp. 475–490.
41. Summer, M.E.; Miller, W.P. Cation Exchange Capacity and Exchange Coefficients. In *Methods of Soil Analysis Part 3. Chemical Methods*; Sparks, D.L., Ed.; Soil Science Society of America Book Series, No. 5; Soil Science Society of America, American Society of Agronomy: Madison, WI, USA, 1996; pp. 1201–1229.
42. Lavkulich, L.M. *Methods Manual: Pedology Laboratory*; Department of Soil Science, University of British Columbia: Vancouver, BC, Canada, 1981.
43. Page, A.L.; Miller, R.H.; Keeney, D.R. *Methods of Soil Analysis (Part 2): Chemical and Microbiological Properties*, 2nd ed.; The American Society of Agronomy: Madison, WI, USA, 1982.
44. De La Mora-Orozco, C.; Flores-Lopez, H.; Rubio-Arias, H.; Chavez-Duran, A.; Ochoa-Rivero, J. Developing a water quality index (WQI) for an irrigation dam. *Int. J. Environ. Res. Public Health* **2017**, *14*, 439. [[CrossRef](#)] [[PubMed](#)]
45. Simsek, C.; Gunduz, O. IWQ index: A GIS-integrated technique to assess irrigation water quality. *Environ. Monit. Assess.* **2007**, *128*, 277–300. [[CrossRef](#)] [[PubMed](#)]
46. Jolliffe, I.T.; Cadima, J. Principal component analysis: A review and recent developments. *Philos. Trans. A Math. Phys. Eng. Sci.* **2016**, *374*, 20150202. [[CrossRef](#)]
47. Chen, Y.D.; Wang, H.Y.; Zhou, J.M.; Xing, L.; Zhu, B.S.; Zhao, Y.C.; Chen, X.Q. Minimum data set for assessing soil quality in farmland of Northeast China. *Pedosphere* **2013**, *23*, 564–576. [[CrossRef](#)]
48. Jagadamma, S.; Lal, R.; Hoefl, R.G.; Nafziger, E.D.; Adee, E.A. Nitrogen fertilization and cropping system impacts on soil properties and their relationship to crop yield in the central Corn Belt, USA. *Soil Till. Res.* **2008**, *98*, 120–129. [[CrossRef](#)]
49. Imperato, M.; Adamo, P.; Naimo, D.; Arienzo, M.; Stanzione, D.; Violante, P. Spatial distribution of heavy metals in urban soils of Naples city (Italy). *Environ. Pollut.* **2003**, *124*, 247–256. [[CrossRef](#)]
50. McGrath, D.; Zhang, C.; Carton, O.T. Geostatistical analyses and hazard assessment on soil lead in Silvermines area, Ireland. *Environ. Pollut.* **2004**, *127*, 239–248. [[CrossRef](#)]
51. Lee, C.S.L.; Li, X.; Shi, W.; Cheung, S.C.N.; Thornton, I. Metal contamination in urban, suburban, and country park soils of Hong Kong: A study based on GIS and multivariate statistics. *Sci. Total Environ.* **2006**, *356*, 45–61. [[CrossRef](#)]
52. Franzen, D.W.; Peck, T.R. Field soil sampling density for variable rate fertilization. *J. Prod. Agric.* **1995**, *8*, 568–574. [[CrossRef](#)]
53. Weisz, R.; Fleischer, S.; Smilowitz, Z. Map generation in highvalue horticultural integrated pest management: Appropriate interpolation methods for site-specific pest management of Colorado potato beetle (Coleoptera: Chrysomelidae). *J. Econ. Entomol.* **1995**, *88*, 1650–1657. [[CrossRef](#)]
54. Ali, R.R.; Moghanm, F.S. Variation of soil properties over the landforms around Idku lake, Egypt. *Egypt. J. Remote Sens. Space Sci.* **2013**, *16*, 91–101. [[CrossRef](#)]
55. De la Rosa, D.; Cardona, F.; Paneque, G. Evaluación de suelos para diferentes usos agrícolas. Un sistema desarrollado para regiones mediterráneas. *An. Edafol. Agrobiol.* **1977**, *36*, 1100–1112.
56. Elbasiouny, H.; Abowaly, M.; Abu_Alkeir, A.; Gad, A.A. Spatial variation of soil carbon and nitrogen pools by using ordinary kriging method in an area of North Nile Delta, Egypt. *Catena* **2014**, *113*, 70–78. [[CrossRef](#)]
57. Abdel-Fattah, M.K.; Abd-Elmabod, S.K.; Aldosari, A.A.; Elrys, A.S.; Mohamed, E.S. Multivariate Analysis for Assessing Irrigation Water Quality: A Case Study of the Bahr Mouise Canal, Eastern Nile Delta. *Water* **2020**, *12*, 2537. [[CrossRef](#)]
58. Wandruszka, R.V. Phosphorus retention in calcareous soils and the effect of organic matter on its mobility. *Geochem. Trans.* **2006**, *7*, 6. [[CrossRef](#)]
59. Nehrani, S.H.; Askari, M.S.; Saadat, S.; Delavar, M.A.; Taheri, M.; Holden, N.M. Quantification of soil quality under semi-arid agriculture in the northwest of Iran. *Ecol. Indic.* **2020**, *108*, 105770. [[CrossRef](#)]
60. Mohamed, E.S.; Abu-Hashim, M.; Abdelrahman, M.A.; Schütt, B.; Lasaponara, R. Evaluating the effects of human activity over the last decades on the soil organic carbon pool using satellite imagery and GIS techniques in the Nile Delta Area, Egypt. *Sustainability* **2019**, *11*, 2644. [[CrossRef](#)]
61. Zalacáin, D.; Martínez-Pérez, S.; Bienes, R.; García-Díaz, A.; Sastre-Merlín, A. Salt accumulation in soils and plants under reclaimed water irrigation in urban parks of Madrid (Spain). *Agric. Water Manag.* **2019**, *213*, 468–476. [[CrossRef](#)]
62. Qadir, M.; Schubert, S. Degradation processes and nutrient constraints in sodic soils. *Land Degrad. Dev.* **2002**, *13*, 275–294. [[CrossRef](#)]
63. Jacobsen, S.-E.; Jensen, C.R.; Liu, F. Improving crop production in the arid Mediterranean climate. *Field Crops Res.* **2012**, *128*, 34–47. [[CrossRef](#)]
64. Food and Agriculture Organization. Salt-affected soils and their management. In *Soils Bulletin*; Food and Agriculture Organization: Rome, Italy, 1988; p. 39.
65. Chi, C.M.; Zhao, C.W.; Sun, X.J.; Wang, Z.C. Reclamation of saline-sodic soil properties and improvement of rice (*Oriza sativa* L.) growth and yield using desulfurized gypsum in the west of Songnen Plain, northeast China. *Geoderma* **2012**, *187*, 24–30. [[CrossRef](#)]
66. Rasouli, F.; Pouya, A.K.; Karimian, N. Wheat yield and physico-chemical properties of a sodic soil from semi-arid area of Iran as affected by applied gypsum. *Geoderma* **2013**, *193–194*, 246–255. [[CrossRef](#)]
67. Temiz, C.; Cayci, G. The effects of gypsum and mulch applications on reclamation parameters and physical properties of an alkali soil. *Environ. Monit. Assess.* **2018**, *190*, 347. [[CrossRef](#)] [[PubMed](#)]

68. Zakarya, Y.M.; Metwaly, M.M.; AbdelRahman, M.A.E.; Metwalli, M.R.; Koubouris, G. Optimized Land Use through Integrated Land Suitability and GIS Approach in West El-Minia Governorate, Upper Egypt. *Sustainability* **2021**, *13*, 12236. [[CrossRef](#)]
69. Michalopoulos, G.; Kasapi, K.A.; Koubouris, G.; Psarras, G.; Arampatzis, G.; Hatzigiannakis, E.; Kavvadias, V.; Xiloyannis, C.; Montanaro, G.; Malliaraki, S. Adaptation of Mediterranean olive groves to climate change through sustainable cultivation practices. *Climate* **2020**, *8*, 54. [[CrossRef](#)]
70. Leteinturier, B.; Herman, J.; Longueville, F.D.; Quintin, L.; Oger, R. Adaptation of a crop sequence indicator based on a land parcel management system. *Agric. Ecosyst. Environ.* **2006**, *112*, 324–334. [[CrossRef](#)]
71. Singha, C.; Swain, K.C. Land Suitability Evaluation Criteria for Agricultural crop selection: A Review. *Agric. Rev.* **2016**, *37*, 125–132. [[CrossRef](#)]
72. Lenz-Wiedemann, V.I.S.; Klar, C.W.; Schneider, K. Development and test of a crop growth model for application within a Global Change decision support system. *Ecol. Model.* **2010**, *221*, 314–329. [[CrossRef](#)]
73. Lorenz, M.; Fürst, C.; Thiel, E. A methodological approach for deriving regional crop rotations as basis for the assessment of the impact of agricultural strategies using soil erosion as example. *J. Environ. Manag.* **2013**, *127*, S37–S47. [[CrossRef](#)]
74. Abuzaid, A.S.; Jahin, H.S.; Asaad, A.A.; Fadl, M.E.; AbdelRahman, M.A.E.; Scopa, A. Accumulation of Potentially Toxic Metals in Egyptian Alluvial Soils, Berseem Clover (*Trifolium alexandrinum* L.), and Groundwater after Long-Term Wastewater Irrigation. *Agriculture* **2021**, *11*, 713. [[CrossRef](#)]
75. Abuzaid, A.S.; AbdelRahman, M.A.E.; Fadl, M.E.; Scopa, A. Land Degradation Vulnerability Mapping in a Newly-Reclaimed Desert Oasis in a Hyper-Arid Agro-Ecosystem Using AHP and Geospatial Techniques. *Agronomy* **2021**, *11*, 1426. [[CrossRef](#)]
76. AbdelRahman, M.A.E.; Rehab, H.H.; Yossif, T.M.H. Soil fertility assessment for optimal agricultural use using remote sensing and GIS technologies. *Appl. Geomat.* **2021**, *13*, 605–619. [[CrossRef](#)]